Detailed Investigations of the Pump−Probe Spectroscopy of the Equilibrated Solvated Electron in Alcohols

Carlos Silva, Peter K. Walhout,† Philip J. Reid,‡ and Paul F. Barbara*

Department of Chemistry, University of Minnesota, 207 Pleasant Street SE, Minneapolis, Minnesota 55455

Received: January 23, 1998; In Final Form: April 13, 1998

Pump−probe spectroscopy of the *equilibrated* solvated electron in methanol and ethanol has been studied with ∼300 fs time resolution. At low pump power the observed dynamics are assigned to s → p excitation and subsequent relaxation of a *localized* solvated electron. In contrast, at high pump power, two-photon absorption apparently produces mobile "conduction band" electrons, which are subsequently trapped and relax at a remote site from the initial equilibrated electron. The two-photon excitation is also observed to induce an ultrafast proton-transfer reaction from the solvent.

I. Introduction

The solvated electron is rapidly emerging as one of the premier model systems for the exploration of condensed-phase structure and ultrafast molecular dynamics.[1−29] It is leading to a unique convergence of theory and experiment, which is not only offering new insights on some of the central issues in condensed phase dynamics but is also allowing for an evaluation of many of the most promising condensed-phase molecular theoretical/computational techniques. Solvated electrons are unique prototypes for condensed-phase quantum dynamics because the spectral properties are strongly dependent on the surrounding environment.

There is general (although not complete)[30] agreement that the Franck−Condon low-lying electronic states of equilibrated solvated electrons in H_2O, alcohols, and other solvents correspond roughly to "localized" electron configurations resembling those of a particle in a sphere, namely, s- and p-like states. The broad, featureless visible to near-IR absorption band of the solvated electron is assigned to three strongly allowed s → p transitions.[11,31−34] The lack of perfect spherical symmetry, however, makes the "s" and "p" designations nominal at best. The low-lying s and p states are localized by the potential well from the solvent molecules. The upper "conduction band" (CB) states are significantly delocalized, since the energy of these states exceeds the local potential well.

The traditional experimental approach to investigate the ultrafast dynamics of solvated electrons involves a two-pulse pump−probe experiment in which the pump pulse generates the solvated electron by multiphoton ionization of the solvent and the probe pulse monitors the subsequent trapping, solvation, and geminate recombination of the electron.[19−29] One of the most exciting issues from this type of experiment is that some fraction of the initially produced CB electrons are trapped in the p state.[25,35−37] Indeed, the p → s internal conversion is predicted to be a critical rate-limiting component of the solvation process.[36,37] The experimental data are highly consistent with this "quantum-solvation" process.

Much of the current research on the solvated electron is focused on the pump−probe spectroscopy of equilibrated s-like electrons, an experimental approach introduced by our laboratory in 1993.[1] In this three-pulse sequence scheme, solvated electrons are generated by photodetachment or, alternatively, photoionization, with a UV "synthesis" pulse. Following equilibration of excess electrons, a femtosecond "pump" pulse promotes a subset of the s state population to a p state. After a variable delay, a tunable femtosecond laser "probe" pulse measures the subsequent relaxation dynamics, which include solvation in the p and s states, as well as the p → s radiationless decay. For the hydrated electron, dynamics are observed with significant amplitudes on three distinct time scales, i.e., 30−70 fs, ∼300 fs, and ∼1 ps.[4] Compared to the two-pulse electron experiment, the three-pulse approach has several advantages, including the absence of complications due to geminate electron−hole recombination, a better defined initial excited electron configuration, and greater theoretical accessibility.

The two- and three-pulse ultrafast dynamics of solvated electrons in alcohols (the subject of this paper) are closely analogous to those of the hydrated electron, which has been more extensively studied by experiment and theory. For the hydrated electron, and for the electron in alcohols, there is an unfortunate ambiguity with respect to the exact interpretation of the ultrafast data, due to overlapping s → p and p → CB transitions in the near-IR and visible wavelength range. Owing to the overlapping transitions, multiple physical mechanisms could account for the observed dynamics. For example, a kinetic model in which photoexcited excess electrons undergo rapid (330 fs) p → s radiationless decay followed by ground-state solvation (1.1 ps) was proposed based on a global fit of hydrated electron three-pulse data (300 fs resolution) over a broad probe wavelength range:[2]

$$s_{eq} \xrightarrow{h\nu} p \xrightarrow[\text{radiationless transition}]{330\ \text{fs}} s_{hot} \xrightarrow[\text{adiabatic solvation}]{1.1\ \text{ps}} s_{eq} \qquad (1)$$

where the subscripts "eq" and "hot" refer to nuclear degrees of freedom and denote equilibrated and nonequilibrated states, respectively.

A contrasting picture emerged for the hydrated electron from quantum molecular dynamics (MD) simulations by Rossky and co-workers.[6−8] In the simulations an equilibrated s state electron

* To whom correspondence should be addressed (barbara@chem.umn.edu).

† Present address: Department of Chemistry, University of Wisconsin, Madison, WI 53706.

‡ Present address: Department of Chemistry, University of Washington, Seattle, WA 98195.

S1089-5639(98)00861-5 CCC: $15.00 © 1998 American Chemical Society
Published on Web 05/15/1998

is "photoexcited" to a p state, and the adiabatic and nonadiabatic relaxation following the vertical (Franck−Condon) transition is monitored. Absorption transients, in good agreement with experimentally measured ones, were constructed from the simulation.[7] The complicated nonmonotonic dynamics are predicted to be the result of the complex evolution of the excited-state spectrum. After the nonadiabatic jump the ground-state equilibrium spectrum is established rapidly compared to the experimental time resolution of ∼300 fs:

$$s_{eq} \xrightarrow{h\nu} p_{fc} \xrightarrow[\text{adiabatic solvation}]{25-300\text{ fs}} p_{eq} \xrightarrow[\text{nonadiabatic transition}]{\sim 1\text{ ps}} s_{hot} \xrightarrow{\ll 300\text{ fs}} s_{eq} \qquad (2)$$

where the subscripts "fc", "eq", and "hot" again refer to nuclear degrees of freedom and represent Franck−Condon, equilibrated, and nonequilibrated states, respectively. The ∼0.3 ps dynamics were interpreted as adiabatic relaxation in the p state. The longer components were assigned to the p → s nonadiabatic decay process. According to the model, the rate-limiting process for the downward nonadiabatic transition is the gradual decrease of the s−p quantum energy gap through solvation dynamics, in response to the new p state shape and charge distribution following photoexcitation.[6] Recent applications of a statistical theory of pump−probe spectroscopy of the hydrated electron by Bratos, Borgis, and co-workers lead to a similar interpretation.[12,13]

It should be emphasized that according to theory, the p state is localized in the original potential well that had trapped the s_{eq}. Although solvent fluctuations could in principle cause the p-state electron to migrate to a remote site in the liquid, simulations for the hydrated electron predict that this is too slow to compete with the p → s radiationless decay in the original site.[6,38]

Yet a third hypothetical interpretation of the three-pulse solvated electron data involves site ejection (detrapping) of the excess electron from the original site by a two-photon mechanism as follows:[39]

$$s_{eq} \xrightarrow{2h\nu} CB \xrightarrow[\text{trapping}]{} p' \xrightarrow[\text{radiationless relaxation}]{\text{solvent dependent}} s_{eq}' \qquad (3)$$

where the subscripts are the same as in eqs 1 and 2 and the prime represents an s or p state electron at a site different from that occupied by the initial equilibrated s-state electron. This interpretation ascribes the observed dynamics in the three-pulse experiment to electron retrapping and solvation at a new site, in analogy to the dynamics of the standard two-pulse electron injection experiment. (Theoretical calculations suggest that near-IR one-photon excitation does not have sufficient energy to directly detrap the electron in water[6] or methanol.[11])

This paper is concerned with a detailed investigation of the three-pulse pump−probe spectroscopy of the solvated electron in methanol and ethanol solvents as a function of probe wavelength in the visible and near-IR and as a function of pump intensity. The results lead to new insights into the validity of the alternative models (eqs 1−3) for the dynamics of the electron in alcohols. The ultrafast data at low pump intensity (one-photon excitation) are consistent with localized p and s states. In contrast, at high pump powers the ultrafast data show evidence of a two-photon channel involving detrapping/retrapping of the solvated electron. The data also lead to new insights of a previously observed excited-state proton-transfer reaction of the solvated electron in alcohols.

II. Experimental Section

A detailed description of the ultrafast transient absorption spectrometer has been given previously.[40] Briefly, a Ti:sapphire-based regenerative amplified laser system produced 130 fs, 180 μJ pulses, centered at 780 nm, at a repetition rate of 2 kHz. Excess electrons were generated using one of two techniques. With the first method the second harmonic of the output of the amplified Ti:sapphire output (390 nm) photoionized I^- in solution. Alternatively, the fourth harmonic of a Q-switched Nd:YLF laser (263.5 nm) produced solvated electrons by photodetachment from α-naphtholate. After a delay of several nanoseconds the resulting equilibrated, ground-state electrons were photoexcited by a 780 nm, 0.3−5 μJ, 130 fs "pump" pulse. A variably delayed, tunable (430−1150 nm) "probe" pulse measured the subsequent relaxation dynamics. The tunability of the probe wavelength was achieved using white-light continuum generated in quartz and selecting a 20 nm portion from the continuum with a computer-controlled variable interference filter wheel. Typical pump and probe spot sizes were 80 and ∼20 μm, respectively.

All solutions were circulated in a 1 mm path flow cell such that each laser pulse sequence encountered a fresh sample region. To avoid accumulation of unwanted species, the sample reservoir was changed frequently. The transients at some wavelengths were corrected for small artifactual signals centered at zero delay caused by pump-induced phase modulation of the probe. In most cases the amplitude of this "artifact" was less than 10% of the signal amplitude. As expected with an absence of complications due to I^-/solvated electron interactions, the initial bleach amplitude was observed to depend linearly on salt (KI or TBAI) concentration, and the normalized transients at low to moderate salt concentrations were found to be superimposable. When I^- at large concentrations (>250 mM) was used as a precursor, there was evidence for I_2^- formation by the diffusive combination of I^- and $I^•$. I_2^- is known to absorb in the same spectral region as the solvated electron and is a potential complication.[41] Addition of a solvated electron quencher (e.g., acetone) to the solution reservoir was observed to completely quench the solvated electron signal and verified that the reported data were not due to an impurity. Transients were also found to be identical using either KI or TBAI in the femtosecond UV synthesis, demonstrating the lack of counterion effects. Finally, transients using either synthesis technique were found to produce indistinguishable ultrafast dynamics of the solvated electron.

III. Results and Discussion

Overview of the Kinetics. Figure 1 shows pump−probe transients of the solvated electron in methanol at various probe wavelengths. Transients near the ground-state absorption maximum (e.g., parts A and B of Figure 1) display an instrument-limited decrease in optical density (bleach) due to s → p photoexcitation. The decrease in optical density recovers on multiple time scales. Transients at the red edge of the spectrum (e.g., parts G and H of Figure 1) show an increase in optical density at zero delay. At intermediate wavelengths (e.g., parts E and F of Figure 1) the data display nonmonotonic dynamics. The initially decreased optical density rapidly overshoots to become an increased absorption at later delays. The data presumably primarily reflect the dynamics of the p → s radiationless decay along, in principle, with solvation dynamics of the s and p states. However, it is difficult to unambiguously assign the dynamics specifically to these processes, owing to overlapping (s → p and p → CB) transitions, which complicate

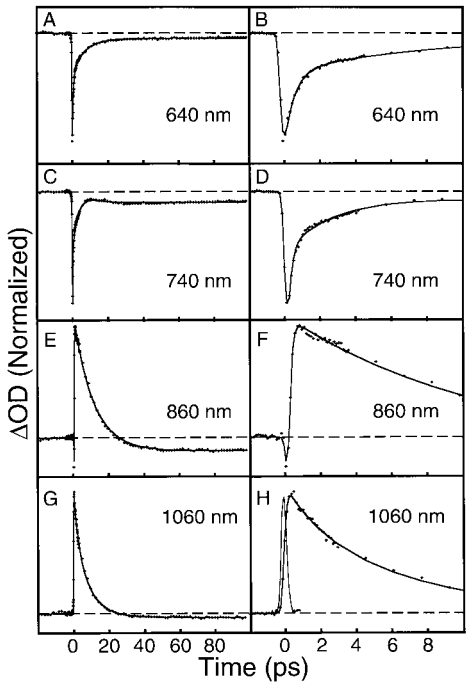

Figure 1. Transient ΔOD (change in optical density) spectra of the solvated electron in 250 mM KI methanol solution obtained at the probe wavelengths indicated in each panel. The solvated electrons were excited with a variably delayed, 780 nm pump pulse and interrogated with a variable wavelength probe pulse. The pump and probe pulses were linearly polarized and oriented at 54.7° (the magic angle) with respect to each other. The first 10 ps of the transient spectra on the left side of the figure are shown on the right side of the figure on an expanded time scale. The solid lines through the data are the multiexponential nonlinear least-squares fit at each wavelength. All fits are convoluted with the instrument response function, shown in the lower right panel.

the interpretation. For example, both the p → CB absorption band and the s → p absorption band (of the unrelaxed s state) may potentially absorb strongly near 1060 nm.[7] Thus, the slow-relaxing transient absorption at 1060 nm may be due to p → s radiationless decay, s-state cooling, or both processes.

The transient ΔOD spectrum of the solvated electron in methanol at various pump−probe delays is shown in Figure 2, further illustrating the trends shown in Figure 1 over the whole spectral region covered by our white-light continuum (430−1150 nm). After only 500 fs following photoexcitation, a significant fraction of the relaxation has already occurred. Within this time scale there is a rapid blue shift in the region from ∼800 to 1150 nm, leading to the nonmonotonic dynamics discussed above. In addition, around the absorption maximum, the initial decrease in optical density recovers by ∼30%. A "pseudo-isosbestic" point emerges close to 800 nm and persists throughout the remaining relaxation.

We have also performed ultrafast transient absorption experiments on the solvated electron in ethanol and ethylene glycol. Table 1 shows multiexponential fits to transients in all of these solvents at a variety of wavelengths.

In addition to the dramatic spectral dynamics due to p → s decay and p- and s-state solvation, there is also a residual bleach at all probe wavelengths that has been previously assigned to an excited-state proton-transfer reaction from the alcohol solvent to the excess electron[3,42−44]

$$s_{eq} + ROH \xrightarrow{h\nu} H^{\bullet} + RO^{-} \qquad (4)$$

This reaction is described in detail below.

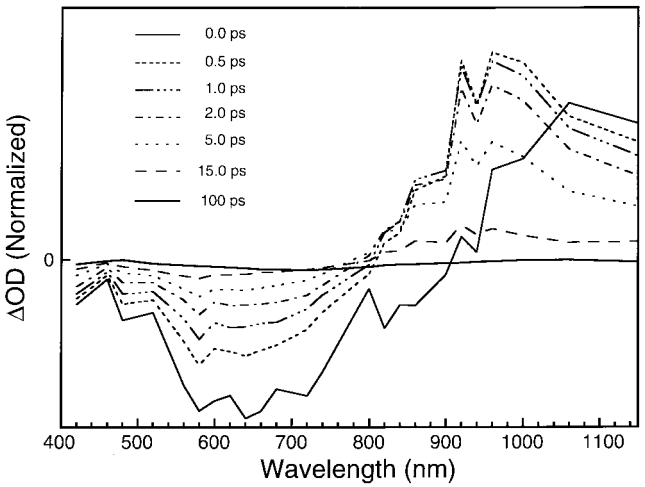

Figure 2. Composite ΔOD spectrum of the solvated electron in 250 mM KI methanol solution at various time delays following excitation with a 780 nm linearly polarized pump pulse oriented at 54.7° with respect to the polarization of the probe pulse. The spectra were reconstructed from the individual transient ΔOD data obtained at 23 different probe wavelengths. Each transient was normalized by scaling the residual bleach at long delays to the equilibrated ground-state absorption cross section at the probe wavelength.

TABLE 1: Multiexponential Fit Parameters for the Transient Pump−Probe Signal of the Solvated Electron in Various Alcohols at Room Temperature[a]

λ (nm)	τ_1 (ps)	A_1	τ_2 (ps)	A_2	τ_3 (ps)	A_3	A_4	$\langle\tau\rangle^b$ (ps)
Methanol (λ_{max} = 640 nm)								
600	0.95	−0.68			9.6	−0.27	−0.050	3.4
640	0.62	−0.68			7.6	−0.27	−0.055	2.6
660	0.44	−0.60			7.2	−0.33	−0.070	2.8
740	0.44	−0.32	5.56	−0.42	6.9	0.21	−0.054	*c*
860	0.22	−0.32	2.74	−0.22	9.9	0.44	−0.018	*c*
950	0.58	−0.46			9.4	0.52	−0.016	*c*
1060	1.0	0.08			10.1	0.91	−0.010	9.3
1150	1.6	0.37			10.7	0.61	−0.015	7.2
Ethanol (λ_{max} = 725 nm)								
680	0.87	−0.58			16.5	−0.37	−0.052	6.9
700	0.42	−0.67			6.1	−0.30	−0.031	2.2
740	0.47	−0.49			8.0	−0.44	−0.074	4.0
860	0.29	−0.79	1.5	−0.08	27.2	0.098	−0.033	*c*
950	1.842	0.64			24.5	0.33	−0.030	9.6
Ethylene Glycol (λ_{max} = 580 nm)								
660	0.42	−0.89			42.3	0.024	−0.084	1.6
800	0.65	−0.51	1.9	0.46	18.5	0.021	−0.0068	2.6
920	0.52	−0.54	3.9	0.25	34.0	0.054	−0.040	9.2

[a] Transients are fit to the function $\Delta OD(t) = \sum_i A_i \exp(-t/\tau_i)$ convoluted with the instrument response function shown in Figure 1H. The amplitudes are normalized such that $\sum_i |A_i| = 1$. τ_4 is always held constant at 100 000 ps to represent a permanent absorption deficit. [b] The average time constant is defined as $\langle\tau\rangle = \sum_i A_i\tau_i/\sum_i A_i$. [c] In the case of transients at probe wavelengths where the dynamics are nonmonotonic, the average time constant is determined using the fit components of the absorptive portion of the transient (i.e., the components with positive amplitude).

Figure 3 shows the dynamics of the solvated electron in normal and deuterated methanol, probing at 660 nm in both cases. Inspection of the data reveals no measurable isotope effect on any portion of the >300 fs dynamics. However, there is a considerable isotope effect on the amplitude of the residual bleach, ascribed to the excited-state proton-transfer reaction (eq 4). At 660 nm, for example, the amplitude of the persistent bleach is ∼7% in MeOH but only ∼2% in MeOD. Table 2 gives multiexponential fit parameters for the solvated electron in

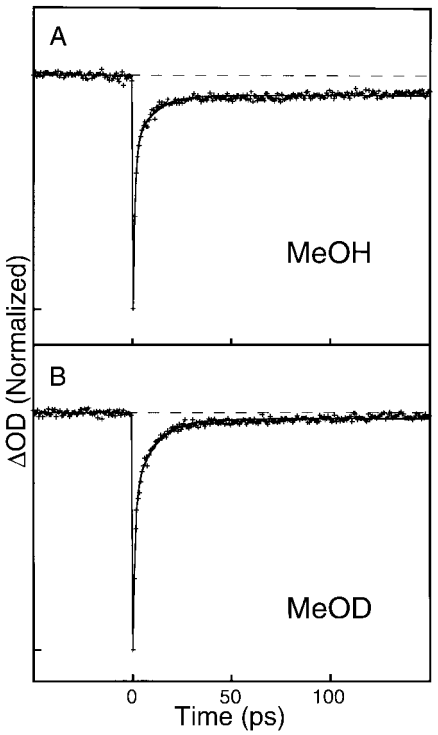

Figure 3. Transient ΔOD spectra of the solvated electron in 250 mM KI methanol (upper panel) and methanol-*d* (lower panel) solutions at 660 nm. The initial ΔOD bleach amplitudes of the methanol and methanol-*d* data sets have been normalized to highlight the differences in the relative residual bleach amplitudes. The solid lines through the data are the multiexponential least-squares fit at each wavelength, convoluted with the instrument response function shown in Figure 1H.

TABLE 2: Multiexponential Fit Parameters for Pump−Probe Measurements of the Solvated Electron in Isotopically Substituted Methanol and Ethanol at Room Temperature[a]

λ (nm)	τ_1 (ps)	A_1	τ_2 (ps)	A_2	τ_3 (ps)	A_3	A_4	$\langle\tau\rangle$[b] (ps)
				Methanol-*d*				
600	0.81	−0.62			12.7	−0.37	−0.018	5.3
660	0.57	−0.64			10.4	−0.33	−0.025	3.9
740	0.52	−0.56			3.59	−0.40	−0.043	1.8
860	0.19	−0.37	2.16	−0.20	10.3	0.43		*c*
950	0.17	−0.31			11.1	0.69		*c*
				Ethanol-*d*				
740	0.85	−0.52			7.3	−0.23	−0.035	2.4
860	0.31	−0.65	1.3	−0.15	21.3	0.17	−0.034	*c*
950	0.30	−0.59	6.8	0.21	28.4	0.17	−0.029	6.6

[a] Transients are fit to the function $\Delta OD(t) = \sum_i A_i \exp(-t/\tau_i)$ convoluted with the instrument response function shown in Figure 1H. The amplitudes are normalized such that $\sum_i |A_i| = 1$. τ_4 is always held constant at 100 000 ps to represent a permanent absorption deficit. [b] The average time constant is defined as $\langle\tau\rangle = \sum_i A_i\tau_i/\sum_i A_i$. [c] In the case of transients at probe wavelengths where the dynamics are nonmonotonic, the average time constant is determined using the fit components of the absorptive portion of the transient (i.e., the components with positive amplitude).

methanol-*d* (MeOD) and ethanol-*d* (EtOD) at a variety of wavelengths.

Pump Power Dependence of the Kinetics. To assign the dynamic processes observed in Figures 1−3 to specific one-photon, two-photon, and higher-order photon-induced processes, we have investigated the ultrafast dynamics as a function of pump pulse energies. Figure 4 displays absorption transients of the solvated electron in ethanol probing at 700 nm (parts A and B) and 950 nm (parts C and D) and pumping with different

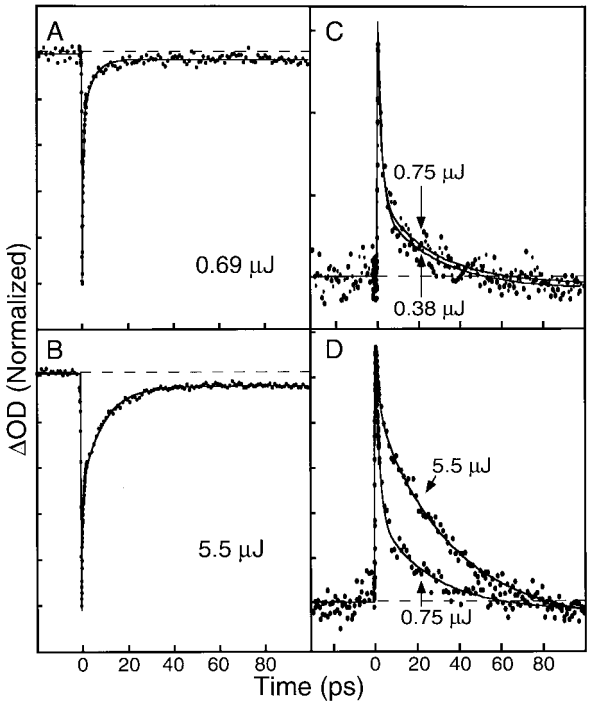

Figure 4. Absorption transient spectra of the solvated electron in ethanol probing at 700 nm using a pump pulse energy of 0.69 μJ (A) and 5.5 μJ (B) and probing at 950 nm with pulse energies of 0.38 and 0.75 μJ (C) and 0.75 and 5.5 μJ (D). The 950 nm data at different powers in panels C and D are superimposed for comparison. In panel C the transients are normalized by the pump intensity, whereas in panel D the transients are normalized to have the same maximum signal. Excess electrons were generated by photodetachment from 10 mM α-naphthol solutions.

pulse energies (indicated in the figure). When the energy of the pump pulse is <1.5 μJ ($\sim$80 μm spot size), the kinetic form of the dynamics is independent of the excitation intensity and the magnitude of the ΔOD signal is linearly proportional to the pump intensity. This is shown in Figure 4C, where two transients at a probe wavelength of 950 nm are obtained by pumping with 0.38 and 0.75 μJ pulses. The data are normalized by the pump pulse energy and are shown to be superimposable. In contrast, at excitation energies larger than $\sim$1.5 μJ, the dynamics become obviously intensity-dependent and the signals do not vary linearly with excitation intensity. Slow-relaxing components become apparent (parts B and D of Figure 4). In Figure 4D the transients are normalized to have the same maximum ΔOD, and *not* by the pump intensity, as in Figure 4C. Therefore, excitation with intense pulses gives access to states that relax on much slower time scales than the one-photon states.

Figure 5A displays how the magnitude of the initial depletion signal at 700 nm (derived from multiexponential fits of the data) depends on pump pulse intensity. At low pump intensities the depletion signal varies linearly, while at higher intensities it shows evidence of saturation, due presumably to excitation of a large fraction of the ground-state electrons. Figure 5A also portrays the pump intensity dependence for the photochemical yield (solid circles in Figure 5A), which is given by the magnitude of the persistent bleach divided by the absorption of the equilibrated electron at 700 nm. The yields show an apparently linear intensity dependence, which at first glance appears to be an indication of a one-photon process. However, the apparently linear intensity dependence does not produce a line going through the origin but rather extrapolates to a negative intercept. Such behavior is expected for a photochemical process resulting from successive two-photon absorption under

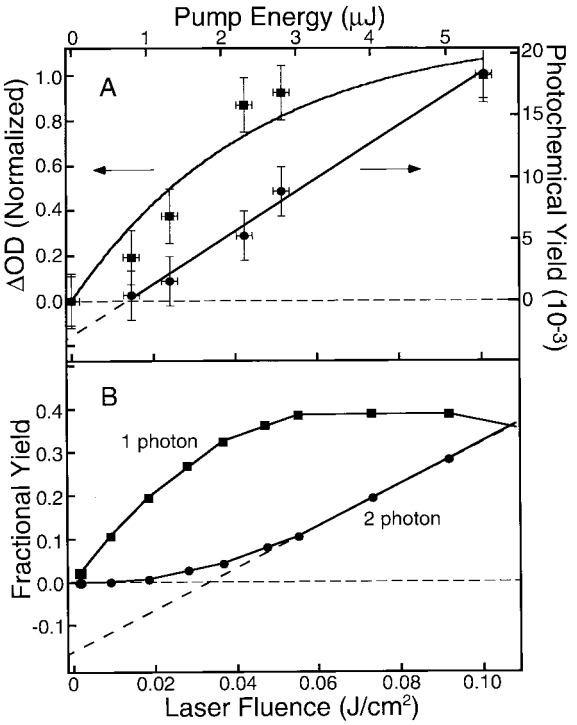

Figure 5. (A) Magnitude of the initial transient ΔOD signal (■) and photochemical yield (●) of the solvated electron in ethanol as a function of excitation fluence, probing at 700 nm. The solid lines are fits to the experimental data. The initial ΔOD signal was fit to the function $\{1 - \exp(-I/I_s)\}$ where I is the intensity and I_s fits to a value of 4.5×10^{-2} J/cm^2. The fit to the photochemical yield is simply a linear function. The magnitude of the initial ΔOD is 3×10^{-3} at the highest pump energy that was investigated. (B) Results of a photodynamical model described in the text. The computed signal components due to one-photon (■) and two-photon (●) processes are displayed. Excess electrons were generated by photodetachment from 5 mM solutions of α-naphthol.

conditions where the first process is easily saturated. This effect is nicely demonstrated by the following simple photodynamic model:

$$s_{eq} \xrightarrow{\sigma_{sp} I_{pu}} p \xrightarrow{\sigma_{pd} I_{pu}} CB \text{ (detrapped)} \quad (5)$$

$$CB + ROH \xrightarrow[\text{proton transfer}]{k_{PT}} RO^- + H^\bullet \quad (6)$$

$$CB \rightarrow p' \text{ and } s' \text{ (retrapped)} \quad (7)$$

Here, σ_{sp} is the cross section for s → p absorption, which is known experimentally, and σ_{pd} is the cross section for the p → CB absorption, which is assumed to be similar to the s → p cross, as suggested by simulations (at least for the hydrated electron).[36,37] We further assume that the pump pulse width is much shorter than the p-state lifetime.

Simulation results from this model are shown in Figure 5B.[45] The line with the solid circles (two-photon channel) represents the fraction of initially equilibrated electrons that are ultimately converted to CB electrons by the pump pulse. The CB electrons subsequently undergo proton transfer or are trapped in a new site. The line with the squares (one-photon channel) correspond to the fraction of initially equilibrated electrons that end up excited in the p state but are not excited by a second photon. At low excitation intensities the one-photon channel dominates, while at higher pump intensities the two-photon channel begins to compete and ultimately dominates (at higher powers than those shown in Figure 5). Since the yield of the two-photon channel at low intensities is very small, an apparently negative intercept is deduced from the experimental yield data (Figure 5A).

The small experimentally observed yield of proton transfer suggests that the branching ratio ($k_{PT}/(k_{PT} + k_T)$) significantly favors trapping over proton transfer. On the basis of the actual PT yield and the simulations in Figure 5B, we estimate the branching ration to be $\sim 10^{-1}$. Assuming that the CB state exists for ~100 fs, which is consistent with simulations, k_{PT} in eq 6 is estimated to $\sim 10^{12}$ s^{-1}. In contrast, the thermally activated proton-transfer reaction between alcohols and s_{eq} is much slower.[46,47] (For example, a pseudo-first-order rate constant of 1×10^5 s^{-1} in ethanol has been reported.[48])

One-Photon-Induced s → p Dynamics. The power dependence that is portrayed in Figures 4 and 5 strongly suggests that the complex pump−probe dynamics of equilibrated electrons in alcohols is generally due to both one- and two-photon excitation under conditions of moderate to high excitation (i.e., >20% of the initial s-state population excited). Nevertheless, in the relatively low-power regime of Figures 1−3 and Table 1, the reported dynamics are predominantly due to one-photon (s → p) excitation.[49]

The relatively fast relaxation dynamics observed for one-photon-excited s_{eq} electrons strongly rules out photodetachment/trapping (eq 3) as a mechanism for this process. Thus, the ultrafast data evidence strongly suggests that the low-power regime kinetics of the solvated electron is indeed due to excitation of s_{eq} to a "localized" p state followed by subsequent relaxation at the original site of s_{eq}, i.e., one of the mechanisms shown in eqs 1 and 2. The ultrafast kinetics of the solvated electron in the extremely slow-relaxing solvent ethylene glycol is consistent with this conclusion. In particular, the observed average relaxation time scale for the photoexcitation in ethylene glycol is orders of magnitude shorter than the expected time scale for relaxation of photoejected electrons.[50]

The new data on the solvated electron do not allow us to distinguish between the related, but distinct, mechanisms represented by eqs 1 and 2. Thus, the slowest component of the observed dynamics at low intensity may either correspond to the p-state lifetime or ground-state solvation time scale. In turn, the faster dynamical processes may be either p state solvation or p → s radiationless decay. Further experiments will be necessary to distinguish between these possibilities.

Two-Photon Excitation of s_{eq}. As mentioned above, at high pump intensities a two-photon channel becomes important in the pump−probe experiment on equilibrated solvated electrons. This two-photon channel is closely analogous to the standard two-pulse photoinjection experiment, as schematically represented in Figure 6. Injected electrons (produced by multiphoton photodetachment) must seek an appropriate trap (e.g., Figure 6A) to localize either in a p state or in the s state.[37] (Excess electrons may be injected into the conduction band or they may be injected through an excited state of the solvent, depending on the photon energy.[22]) Further relaxation processes (the p → s electronic transition, adiabatic solvation) occur on a solvent-dependent time scale. In the pump−probe experiment, two-photon excitation of the solvated electron ejects the electron to the conduction band, where it may retrap in a different site (e.g., site 2 in Figure 6B). The formation of fully equilibrated s′ electrons involves the same relaxation processes as those manifested in the injection experiments. The time scales of the slow component in the high pump intensity regime are very similar to those observed in photoinjection experiments. For example, comparison of our high excitation intensity data with

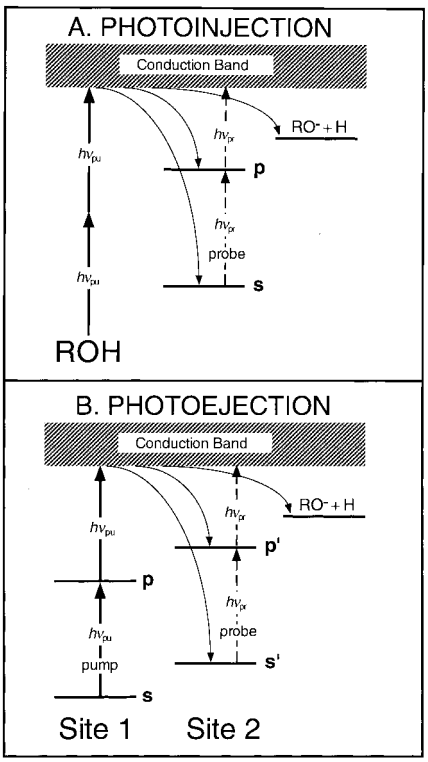

Figure 6. Schematic illustration of one- vs two-photon excitation of the equilibrated solvated electron. (A) In the photoinjection experiment an injected electron is localized in an s or p state. (B) In the photoexcitation experiment one-photon excitation of an s-state electron in site 1 produces a (localized) p-state electron. Two-photon excitation produces a CB electron, which may localize in a distinct site from the original one (site 2). Alternatively, the CB electron may accept a proton from a solvent molecule.

the data from Shi et al. for the solvated electron in methanol and ethanol shows that the dominant kinetic feature in both cases occur on similar time scales (~7 ps in methanol, ~15 ps in ethanol).[23] The dominance of slow components at high pump intensities is also observed for the hydrated electron,[5] although a comparison of pump−probe and the photoinjection experiments is more problematic because of the presence of unsubtractable artifacts and the limited time resolution and signal-to-noise ratio in the published photoinjection data.[24,28] In alcohols, where the time scale for the fast and slow relaxation components observed in the data are better separated, the correspondence between the two- and the (high pump power) three-pulse experiments is clear.

One important distinction between the (one-photon) pump−probe experiment and the photoinjection experiment is the role played by the slow kinetic components, demonstrated by the average relaxation time, $\langle\tau\rangle$. Although the slow components dominate the dynamics following photoinjection, they play a lesser role in the one-photon pump−probe data. (For example in Figure 4D, $\langle\tau\rangle$ is ~9 ps pumping with 0.75 μJ pulses but ~29 ps with 5.5 μJ pulses.) This is an indication that in the low pump-power experiment the large amplitude, slow solvent motions are largely frozen out during the time scale required for the radiationless transition process. They play a critical role, however, in the photoinjection (and multiphoton pump−probe) experiment.

It is interesting to compare the concept of the CB electron with a related concept in radiation chemistry, the "dry" electron. Upon radiolysis of water and alcohols a transient species (the dry electron), with energy well above the thermal energy, is formed.[51] Hunt and co-workers established that the dry electron reacts very efficiently with scavengers in competition with excess electron relaxation and solvation.[52,53] The high quenching efficiency suggested that the dry electron undergoing the reaction is either an extended wave packet or a delocalized particle.[54] Experiments by Lewis and Jonah on the reactions of the dry electron in ethanol and *n*-propanol over a wide temperature range are in agreement with that hypothesis.[55] This leads one to compare the CB electrons prepared in our experiment via two-photon excitation with the highly reactive "dry" electrons discussed in the radiation chemistry literature. This possibility opens up the door for future studies of CB electron structure and dynamics, since climbing the energy ladder from the ground state represents a new way of producing CB electrons.

Solvent Isotope Effects. Another important issue to evaluate the different mechanisms for the transient absorption dynamics presented here is their predictions of solvent isotope effects on the p → s radiationless transition rate. Figure 3 shows that we observe no significant isotope effects on any portion of the dynamics within our time resolution of 300 fs. There are presently no nonadiabatic MD simulations on the solvated electron in methanol to compare predicted isotope effects on the p-state lifetime with the data, but hydrated electron simulations give conflicting predictions. Nonadiabatic MD simulations by Schwartz and Rossky predict that the excited-state lifetime is a factor of ~2 longer in D_2O than in H_2O.[8] This is a result of smaller nuclear velocities in deuterated water, producing a smaller nonadiabatic coupling between the ground and excited states. It was predicted, however, that the decay of quantum coherence after nonadiabatic coupling takes ~50% longer in D_2O than in H_2O, and therefore, the smaller nonadiabatic coupling acts coherently for a longer time than in H_2O.[9,10] After inclusion of this effect in the simulation, only a small net isotope effect on the radiationless transition rate remained. It should be noted that it was argued that the nearly complete cancellation of the dependence of the decoherence time and nonadiabatic coupling in the case of the p → s transition of the hydrated electron is accidental, and a larger isotope effect should be seen in other solvents.[17] A small isotope effect in the lifetime of the p state is in agreement with the data presented in this work but in contrast to predictions from nonadiabatic MD simulations by Neria and Nitzan,[16] which used a golden rule expression to calculate the p → s nonadiabatic decay rate. The nonadiabatic transition time constant was found to be 220 fs in H_2O and ~800 fs in D_2O. A recent study of the pump−probe spectroscopy of the hydrated electron by Bratos, Borgis, and co-workers, using a statistical theory, predicts that an isotope effect should be observed at the wings of the absorption band but not in the vicinity of the excitation frequency.[13] This effect is predicted because near the pump frequency the spectral evolution is dominated by a solvent-independent "coherent spike", which is superimposed on a "thermic band" that dynamically depends on the nonadiabatic rate constant. Since that parameter is solvent-dependent (due to different nuclear velocities), an isotope effect is expected in the evolution of the thermic band. The hydrated electron shows a ~1.4 isotope effect in the Gaussian, ~30−70 fs component of the dynamics near the pump frequency.[4] It is also interesting to compare the experimental results with the hydrodynamic theory of hydrated electron solvation of Rips, which assumes that the excess electron resides in a symmetric cavity in an ideal, incompressible liquid, and the reaction coordinate for the radiationless transition is the cavity radius itself.[18] This simple model predicts that the transition time scale depends on isotopic substitution only through the square root of the solvent density, producing a 5% H_2O/D_2O isotope effect

that is consistent with the experimental observations of the hydrated electron.[4] The square root of the density ratio of methanol and methanol-*d* is 1.01. A ~1% isotope effect is also in agreement with the data presented in this paper.

The isotope effect on the yield of photochemical reaction (eqs 5 and 6) is in agreement with earlier studies in which nanosecond laser pulses photobleached equilibrated solvated electrons, and the loss of absorbance was monitored with a pulsed xenon lamp.[42−44] A large isotope effect was observed in the permanent photobleaching yield, in agreement with the data reported herein. The photochemical yield was altered by deuteration of the hydroxy fragment of the solvent molecules but remained unaffected when other parts of the molecule were deuterated. This is evidence that the OH bond vibration plays a critical role in the photoinduced proton-transfer mechanism.

IV. Conclusions

We report ~300 fs resolved pump−probe spectroscopy of the equilibrated solvated electron in methanol, ethanol, and ethylene glycol over a broad probe wavelength range throughout the visible and in the near-IR regions. The spectral evolution following s → p photoexcitation is complex and reflects the involvement of transient solvation effects in the p → s radiationless decay dynamics of the solvated electron. Pump pulse intensity dependence studies reveal that the complex spectral evolution observed in all solvents is due to a one-photon excitation regime at low pump intensity and a two-photon excitation regime at high pump intensities. The one-photon regime is assigned to excitation and subsequent relaxation between s- and p-like states that are localized in the same solvent "site". In contrast, the two-photon regime is assigned to successive two-photon excitation of the electron, producing conduction band electrons that ultimately are trapped at new solvent sites. Additionally, the CB electrons are observed to decay via a reactive channel that has been ascribed to a proton-transfer reaction between the conduction band electron and the alcohol solvent molecules. A lower limit of ~300 fs for the p-state lifetime after photoexcitation is established for the solvated electron in methanol. Lifetimes as long as tens of picoseconds are not ruled out by the analysis reported herein. Experiments performed in methanol-*d* and ethanol-*d* reveal that within the time resolution of these experiments (~300 fs), no observable isotope effect is present in any kinetic component except in the yield of the photoinduced proton-transfer reaction. These results provide an important step toward an understanding of the electron photoinjection and the pump−probe experiments in alcohols.

Acknowledgment. This research was supported by a grant from the DOE-BES.

References and Notes

(1) Alfano, J. C.; Walhout, P. K.; Kimura, Y.; Barbara, P. F. *J. Chem. Phys.* **1993**, *98*, 5996.
(2) Kimura, Y.; Alfano, J. C.; Walhout, P. K.; Barbara, P. F. *J. Phys. Chem.* **1994**, *98*, 3450.
(3) Walhout, P. K.; Alfano, J. C.; Kimura, Y.; Silva, C.; Reid, P. J.; Barbara, P. F. *Chem. Phys. Lett.* **1995**, *232*, 135.
(4) Silva, C.; Walhout, P. K.; Yokoyama, K.; Barbara, P. F. *Phys. Rev. Lett.* **1998**, *80*, 1086.
(5) Yokoyama, K.; Silva, C.; Son, D.; Walhout, P. K.; Barbara, P. F. *J. Phys. Chem. A*, submitted.
(6) Schwartz, B. J.; Rossky, P. J. *J. Chem. Phys.* **1994**, *101*, 6902.
(7) Schwartz, B. J.; Rossky, P. J. *J. Chem. Phys.* **1994**, *101*, 6917.
(8) Schwartz, B. J.; Rossky, P. J. *J. Chem. Phys.* **1996**, *105*, 6997.
(9) Schwartz, B. J.; Bittner, E. R.; Prezhdo, O. V.; Rossky, P. J. *J. Chem. Phys.* **1996**, *104*, 5942.
(10) Prezhdo, O. V.; Rossky, P. J. *J. Chem. Phys.* **1997**, *107*, 5863.
(11) Turi, L.; Mosyak, A.; Rossky, P. J. *J. Chem. Phys.* **1997**, *107*, 1970.
(12) Bratos, S.; Leicknam, J.-C. *Chem. Phys. Lett.* **1996**, *261*, 117.
(13) Bratos, S.; Leicknam, J.-C.; Borgis, D.; Staib, A. *Phys. Rev. E* **1997**, *55*, 7217.
(14) Staib, A.; Borgis, D. *J. Chem. Phys.* **1995**, *103*, 2642.
(15) Barnett, R. B.; Landman, U.; Nitzan, A. *J. Chem. Phys.* **1989**, *90*, 4413.
(16) Neria, E.; Nitzan, A. *J. Chem. Phys.* **1993**, *99*, 1109.
(17) Graf, P.; Nitzan, A.; Diercksen, G. H. F. *J. Phys. Chem.* **1996**, *100*, 18916.
(18) Rips, I. *Chem. Phys. Lett.* **1995**, *245*, 79.
(19) Sander, M.; Brummund, U.; Luther, K.; Troe, J. *Ber. Bunsen-Ges. Phys. Chem.* **1992**, *96*, 1486.
(20) Sander, M. U.; Luther, K.; Troe, J. *J. Phys. Chem.* **1993**, *97*, 11489.
(21) Reuther, A.; Laubereau, A.; Nikogosyan, D. N. *J. Phys. Chem.* **1996**, *100*, 16794.
(22) Crowell, R. A.; Bartels, D. M. *J. Phys. Chem.* **1996**, *100*, 17940.
(23) Shi, X.; Long, F. H.; Lu, H.; Eisenthal, K. B. *J. Phys. Chem.* **1995**, *99*, 6917.
(24) Shi, X.; Long, F. H.; Lu, H.; Eisenthal, K. B. *J. Phys. Chem.* **1996**, *100*, 11903.
(25) Migus, A.; Gauduel, Y.; Martin, J. L.; Antonetti, A. *Phys. Rev. Lett.* **1987**, *58*, 1559.
(26) Mcgowen, J. L.; Ajo, H. M.; Zhang, J. Z.; Schwartz, B. J. *Chem. Phys. Lett.* **1994**, *231*, 504.
(27) Pépin, C.; Goulet, T.; Houde, D.; Jay-Gerin, J.-P. *J. Phys. Chem.* **1994**, *98*, 7009.
(28) Pépin, C.; Goulet, T.; Houde, D.; Jay-Gerin, J. P. *J. Phys. Chem. A* **1997**, *101*, 4351.
(29) Turi, L.; Holpar, P.; Keszei, E.; Pépin, C.; Houde, D. *J. Phys. Chem. A* **1997**, *101*, 5469.
(30) Tuttle, T. R.; Golden, S. *J. Phys. Chem.* **1991**, *95*, 5725.
(31) Spirk, M.; Impey, R. W.; Klein, M. L. *J. Stat. Phys.* **1986**, *43*, 967.
(32) Schnitker, J.; Motakabbir, K.; Rossky, P. J.; Friesner, R. *Phys. Rev. Lett.* **1988**, *60*, 456.
(33) Wallqvist, A.; Martyna, G.; Berne, B. J. *J. Phys. Chem.* **1988**, *92*, 1721.
(34) Romero, C.; Jonah, C. D. *J. Chem. Phys.* **1989**, *90*, 1877.
(35) Long, F. H.; Lu, H.; Eisenthal, K. B. *Phys. Rev. Lett.* **1990**, *64*, 1469.
(36) Webster, F. J.; Schnitker, J.; Friedrichs, M. S.; Friesner, R. A.; Rossky, P. J. *Phys. Rev. Lett.* **1991**, *66*, 3172.
(37) Murphrey, T. H.; Rossky, P. J. *J. Chem. Phys.* **1993**, *99*, 515.
(38) Del Buono, G. S.; Rossky, P. J.; Murphrey, T. H. *J. Phys. Chem.* **1992**, *96*, 7761.
(39) Goulet, T. Private communication.
(40) Kliner, D. A. V.; Alfano, J. C.; Barbara, P. F. *J. Chem. Phys.* **1993**, *98*, 5375.
(41) Walhout, P. K.; Alfano, J. C.; Thakur, K. A. M.; Barbara, P. F. *J. Phys. Chem.* **1995**, *99*, 7568.
(42) Shida, T.; Imamura, M. *J. Phys. Chem.* **1974**, *78*, 232.
(43) Bromberg, A.; Thomas, J. K. *J. Chem. Phys.* **1975**, *63*, 2124.
(44) Kenney-Wallace, G. A.; Hall, G. E.; Hunt, L. A.; Sarantidis, K. *J. Phys. Chem.* **1980**, *84*, 1145.
(45) The photodynamical model consists of first-order kinetic processes representing excitation of a fraction of the initial s-state population to a p state by a Gaussian optical pulse (standard deviation = 100 fs), absorption of the p state, and radiationless decay from the p state with a 1 ps lifetime. Stimulated emission is neglected, since it is not expected to participate in the >300 fs dynamics in this wavelength range (see ref 6). After the time-dependent populations are calculated, the total change in optical density at the probe wavelength is determined and the results are convoluted with a Gaussian probe pulse. Spatial integration along the pump beam profile does not significantly change the results due to the relative pump and probe spot sizes.
(46) Fowles, P. *Trans. Faraday Soc.* **1971**, *67*, 428.
(47) Matsumura, H.; Mafuné, F.; Kondow, T. *J. Phys. Chem.* **1995**, *99*, 5861.
(48) Farhataziz; Kalachandra, S. *IEEE Trans. Nucl. Sci.* **1983**, *NS-30*, 1645.
(49) Indeed, previously published data on the solvated electron in alcohols (see ref 3) may be in the moderate excitation regime and are presumably partly contaminated by two-photon effects.
(50) Horng, M. L.; Gardecki, J. A.; Papazyan, A.; Maroncelli, M. *J. Phys. Chem.* **1995**, *99*, 17311.
(51) Jonah, C. D.; Bartels, D. M.; Chernovitz, A. C. *Radiat. Phys. Chem.* **1989**, *34*, 145.
(52) Wolff, R. K.; Bronskill, M. J.; Aldrich, J. E.; Hunt, J. W. *J. Phys. Chem.* **1973**, *77*, 1350.
(53) Lam, K. Y.; Hunt, J. W. *Int. J. Radiat. Phys. Chem.* **1975**, *7*, 317.
(54) Razem, D.; Hamill, W. H.; Funabashi, K. *Chem. Phys. Lett.* **1978**, *53*, 84.
(55) Lewis, M. A.; Jonah, C. D. *J. Phys. Chem.* **1986**, *90*, 5367.